STATE OF THE ART REPORT

Path Planning of an Unmanned Aerial Vehicle (UAV) with Minimal Energy Consumption

Submitted by

Paraj Ganchaudhuri

Roll No.: 206102023

Under the guidance of

Dr. Chayan Bhawal

Department of Electronics and Electrical Engineering

Indian Institute of Technology Guwahati

Guwahati - 781039, Assam, India

April 2022

Abstract

Unmanned Aerial Vehicle (UAV) or drone constitutes a new workforce in modern transportation system for delivery and surveilance operations. There are various other use cases for an UAV but a fundamental drawback in its application is its limited flight time. One of the well-known problem in this area is towards optimal path planning of an UAV with minimal energy and or minimal time of operation. Energy/Power consumption modeling of an UAV is a critical tool for evaluating path planning of an UAV. However, there are multiple parameters that add to the power which is not easy to identify and track in general and as a result, there are inaccuracies in the calculation of power. In this research we make an attempt to map the dynamics/environment and maneuvers of a drone to angular speeds of the rotors as rotors are the end consumers of power in an UAV. Using the speeds, we try to obtain a power model which can calculate the energy that will be required for a trip. The power model will also be able to track dynamic uncertainties. We also intend to redesign a path planning algorithm that can handle dynamically evolving environments and provide the operator with optimal routes even when the UAV faces external disturbances or there is a change in objective of the UAV in mid-flight.

Contents

List of Figures

1 Introduction

Unmanned Aerial Vehicles (UAVs) or drones over the years have found widespread application in the field of robotics viz., surveillance in remote areas, precision farming, logistics, emergency responsiveness, etc. Such applications of UAVs have led to a massive boom in the UAV market worldwide. In India, The Civil Aviation Ministry estimates India's drone sector to achieve a total turnover of Rs. 120-150 billion (US$ 1.63-2.04 billion) by 2026 [1]. The major areas where UAVs are projected to make massive footprints are:

1. Surveillance - India has 15,106.7 km of international land border and a coastline of 7,516.6 km that are of potential importance for surveillance. Present surveillance infrastructure is both fuel-inefficient and manpower intensive. So, there is an immense space yet to be filled by UAVs [2].

2. Precision Agriculture - India has arable lands with over 155 million hectares, and it amounts to approximately $265 billion worth of revenue. UAVs can be an important tool to provide leading-edge digital and precision agriculture technologies to farmers to maximize the efficient use of water, fertilizer and pesticides and improve overall productivity, quality, and yield [3].

Such widespread applications have also led to a bureaucratic push in the country to promote UAVs' use in various sectors. Hence rules and regulations on licensing and commercial use has been preferentially eased out [4].

Considering the importance of this industry, research into UAVs for various applications has been actively pursued by the research community[5]. Among the various research areas on UAVs, in this project, we focus on the problem of path planning for UAVs in a dynamically evolving environment with an emphasis on minimal energy consumption.

One of the most sought-after features in most applications involving UAVs is to increase flight time by decreasing the consumption of energy. Hence we perform path planning to identify the path with minimum energy. To evaluate the energy comsumption of a path, we require a power consumption model and in practical scenerious it is very tough to derive a perfect model because there are multiple parameters at play which contribute to power consumption. Also, these paramters are difficult to identify and track in general. In most cases the power model can only capture straight line paths of UAVs with no role of external disturbances(wind). Based on the available literature, different models results different values of power for idetical UAV operations with identical hardwares. So, there is no consensus in the available powoer modelings[6].

So here, in this project, we make an attempt to derive a power consumption model that can translate the role of various parameters into fewer and most important ones which will be easy to track and evaluate. We also aim to track the dynamic power consumptio of the UAV with its various manuevers as well as map the power variations when there are disturbances(wind).

With the help of a power formulation, we aim to calculate the energy that will be consumed for a given trip/operation and perform path planning with some objectives. In most cases, to the best of my knowledge, for a given objective, the trajectories for each agent (say in parcel delivery) are computed offline. This approach does not factor in the external uncertainties on the energy consumption modeling. Such uncertainties may include communication delays, localization information loss (GPS-denied environment) etc. In the middle of a flight, there might also be a change in objective for a UAV. Thus,

research pertaining to path planning with a dynamically evolving environment/objective is another problem we wish to address with this research.
This report is divided into two sections. At first we study various power consumption models available in literature and find out significant research gaps. Then we introduce a power model based on angular speeds of the rotors. Next we study about the various path planning formalisms to achieve optimal paths for a given UAV operation.

2 Power Consumption Modeling

The major parameters that affect power consumption of an UAV are summarised below [6], [7], [8]

UAV Design	**Environment**	**Drone dynamics**	**Delivery operations**
UAV weight	Air density	Airspeed (vertical and horizontal)	Payload weight
Number of rotors	Gravity	Motion (take-off/landing/ hover/levelled flight)	Size of payload
Number of blades per rotor	Wind velocity	Acceleration/ Deacceleration	Drag coefficient of payload
Total propeller area	Wind incident angle	Roll/pitch/yaw angle	Fleet size and mix
Blade chord length	Weather (rain, snow etc.)	Angular speed of rotors	Single/multi stop trip
Angle of attack of propeller disk	Ambient temperature	Flight angle	Delivery mode (tether/landing/ parachute)
Advance ratio of propeller	Regulations	Flight altitude	Area of service region
Size of rotors			
Size of drone body			
UAV body drag co-efficients			
Battery weight			
Battery energy capacity			
Size of battery			
Power transfer efficiency			
Maximum speed			
Maximum payload			
Lift-to-drag ratio			
Delivery mechanism			
Avionics			

2.1 Literature Survey on power consumption modeling

- D'Andrea in [9] provides an influential contribution to model power consumption of an UAV by translating the fundamental flight principles of manned aircraft to a model for the much smaller scale of unmanned aerial drones. [9] presents a model using an integrated approach that combines aerodynamic and drone design aspects into a single critical parameter: the lift-to-drag ratio r. The energy model also includes a fixed component for avionics power. Using the fact that a high-end lithium-ion battery has a specific power of 0.35 kW/kg, the paper proposes a metric to obtain the required battery weight for a trip. The worst-case energy requirement in kWh is formulated and economics i.e the average energy cost per kilometer is also addressed. Lastly, the average battery cost per km is approximated for a trip given a payload weight and flight velocity.

- Dorling et al. in [8] provides an equation for the power that is consumed by a multirotor helicopter in hover as a function of the battery and payload weight. The approach for this modeling is based on helicopter operations, with the assumption that the power consumed during level flight, takeoff, or landing is approximately equivalent to the power consumed while hovering as the power consumed by the helicopter is often reduced due to translational lift, a phenomenon where air flowing horizontally along the rotor generates additional lift. This power consumption model does not consider the role of UAV speed. These authors also report field experiments on a 3D Robotics ArduCopter Hexa-B hexacopter. and develop regression parameters with small payloads.

- In [7], Liu et al. derive a power consumption model where power is distributed into three components namely induced power, profile power, and parasitic power. The power generated by the propellers to balance the weight of the UAV in flight is represented by induced power. Profile power overcomes the rotational drag encountered by rotating propeller blades. The parasite power resists body drag when there is relative translational motion between the vehicle and wind. These power equations are derived analytically using aerodynamic principles and then encapsulated with fewer parameters. The values of these parameters are obtained by conducting field tests on an IRIS+ UAV. A least-square fit for power vs payload is also obtained. It is shown that ascending takes 9.8% more power than hovering, and descending takes 8.5% less power than hovering.

- Kirchstein in [10] derives component-based model similar to [7] but specifically for a drone delivery application. He describes characteristic power consumption calculations for takeoff and ascent, steady level flight, descent, hovering, and landing. The return trip is considered similar but without the payload. Kirchstein also compares delivery with trucks versus UAVs in Berlin and shows that drone delivery often requires more energy. The article also shows how wind and drone hovering increase the power consumption of an UAV. It is concluded that in rural settings with long distances between customers, UAV-based parcel delivery infrastructure has comparable energy considerations to a delivery system with electric trucks.

- The authors in [11] studied a truck-drone hybrid delivery system. In this study, they extend vehicle routing models to the hybrid delivery systems by taking into account two important practical issues: the effect of parcel weight on drone energy

consumption and restricted flying areas. The power consumption model is derived from [8] and tweaked to obtain the flight time of an UAV for an operation. They obtain a formulation where the variation in flight time is obtained based on the variation in the payload. The model is tested against practical experiments on an MK8-3500 standard UAV and it is claimed that the results are realistic.

- Tseng et al. in [12] uses a black-box modeling approach to obtain the power consumption model of an UAV. Field experiments are performed by the researchers considering the impact of various flight scenarios, payload weight and wind to study how power consumption varies with them, and then a non-linear regression model is presented. They obtain the power model where horizontal and vertical speed and acceleration, as well as payload mass and wind speed, are the variables. It is also mentioned that the error in estimation of power consumption in the field experiments is within 0.4% of the original power consumption obtained from the onboard sensors.

- In [13], Stolaroff et al. develops a two-component model based on the thrust required to balance the UAV weight and the parasite drag force. The power consumption model is derived for hovering from helicopter dynamics like [8] and then extended for steady flight for variation with significant velocity or in significant wind. The minimum power requirement then changes somewhat depending on the airspeed and incident angle at which the UAV traverses. This model is used to assess the energy use and life cycle greenhouse gas (GHG) emissions for small drones with short ranges (4 km) delivering from warehouses. Results indicate that small drones are likely to provide lower lifecycle GHG emissions than conventional delivery trucks, but that benefits depend on the carbon intensity of electricity and the size of the drones.

- Zhang et. al in [6] studies the significant power models available in literature and reviews, classifies the drone energy, consumption models. They document very wide variations in the modeled energy consumption rates resulting from differences in the scopes and features of the models, the specific designs of the drones; and the details of their assumed operations and uses. They also try to obtain the optimum value of payload weight and flight speed that would minimize the energy consumed per unit distance on a few standard energy consumption models.

We have collated the results and have elaborated various types of power consumption model in the next section

2.2 Types of Power Consumption Modeling

There are various approaches available in the literature for modeling the power consumed by an UAV. Different approaches of modeling along with some significant Power Consumption Model(PCM) are studied below.

2.2.1 Component based power modeling

For such a modeling, the flight paths are assumed to consist of a vertical-take-off segment, hover, a combination of horizontal straight line segments for levelled flights, and a vertical-landing segment. Based on [7], power consumed by a multi-rotor UAV is

distributed into three components, namely induced power (P_i), profile power (P_p) and parasitic power (P_{par}).
The following symbols will be required to define the different notions of power in component based modeling

- T : Total thrust applied by the UAV
- k_1 : Ratio of actual airflow to idealised uniform airflow
- ρ : Density of air
- A : Total propeller area
- V_{vert} : Vertical velocity of the UAV
- V_{air} : Horizontal velocity of the UAV
- N : Total number of blades in a single propeller
- M : Total number of rotors
- c_d : Drag coefficient of the blade
- c : Blade chord width
- C_d : Drag coefficient of vehicle body
- R : Radius of the propeller blade
- ω_i : Angular speed of i^{th} rotor
- μ_i : Advance ratio for propellers in rotor i
- α_i : Angle of attack for propeller disks in rotor i
- V_{wind} : Velocity of wind head on to the UAV
- V_{ground} : Ground velocity of the UAV
- A_{quad} : Cross sectional area of the vehicle when against wind
- c_l : Lift coefficient

1. Induced Power - The induced power is the power required to keep the UAV afloat. The modeling of induced power is derived from disk actuator theory [14].

$$P_i = k_1 T \left(\sqrt{\frac{T}{2\rho A} + \left(\frac{V_{vert}}{2}\right)^2} + \frac{V_{vert}}{2} \right) \tag{1}$$

2. Profile Power - The profile power is the power required to overcome the rotational drag encountered by rotating propeller blades. The profile power consumed by a

rotating rotor blade is derived from blade element theory [15]. The profile power for the i^{th} rotor while the UAV is hovering is given by

$$P_{p,hover,i} = \frac{N \times c \times c_d \times \rho \times R^4}{8} {\omega_i}^3 \tag{2}$$

During horizontal flight, the profile power becomes

$$P_{p,i} = P_{p,hover,i} \left(1 + {\mu_i}^2\right) \tag{3}$$

where,

$$\mu_i = \frac{V_{air} cos(\alpha_i)}{\omega_i R} \tag{4}$$

In addition, all angles of attack are identical. Then the total profile power is

$$P_p = \sum_{i=1}^{M} P_{p,i} = \sum_{i=1}^{M} \left(\frac{N \times c \times c_d \times R^4}{8} {\omega_i}^3 \left(1 + {\mu_i}^2\right) \right) \tag{5}$$

$$P_p = \sum_{i=1}^{M} \left(\frac{N \times c \times c_d \times \rho \times R^4}{8} \left({\omega_i}^3 + \left(\frac{V_{air} cos(\alpha_i)}{R} \right)^2 \omega_i \right) \right) \tag{6}$$

3. Parasitic Power - The parasite power is the power required to resist body drag when there is relative translational motion between the vehicle and wind. The parasite power is obtained by assuming that the body drag (F_{par}) is proportional to airspeed (V_{air}) squared.

$$P_{par} = \frac{1}{2} C_d \times \rho \times A_{quad} \times {V_{air}}^3 \tag{7}$$

These power equations are applicable only when the UAV is at steady state, i.e in force equilibrium. Figure 1 shows all the external forces, where

- L is the lift
- D is the parasitic drag
- α is the angle of attack

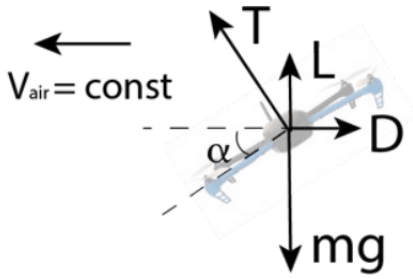

Figure 1: The UAV under force equilibrium in horizontal and vertical directions

Therefore, the thrust at steady state is computed from

$$T = \sqrt{(mg - L)^2 + D^2} \tag{8}$$

The lift as described in [7] is given by

$$L = c_5(V_{air}cos\alpha)^2 + c_6T \tag{9}$$

where $c_5 = \frac{N \times c \times c_l \times \rho \times R}{4}$ and $c_6 = k_3\frac{N \times c \times c_l \times \rho \times R^3}{6}$.

$$D = c_4V_{air}^2 \tag{10}$$

where $c_4 = \frac{C_d \times \rho \times A_{quad}}{2}$
Theoretically, solution for T can be obtained by solving a complicated quadratic equation, by substituting equation eq(9) into eq(8). However, we are only interested in modeling lift as a function of horizontal airspeed. It allows us to match the thrust reduction observed in horizontal flight. Therefore, it is further assumed that $c_6 = 0$, to simplify the identification process.

Simplified analytical expressions for Power The power consumed by an UAV needs to be calculated using the powers that are described above. From equations eq(1), eq(6) and eq(7) it is evident that there are a lot of parameters at play and it is not convenient to have an exact estimation of all the parameters during every operation. The parameters that are dependent on an UAV operation are Thrust T which is a measure of the weight carried by the UAV, V_{air}, the horizontal speed and V_{vert}, the vertical speed of the UAV.
So a power equation needs to be formulated based on these variables. Accordingly, eq(1), eq(6) and eq(7) can be encapsulated as

$$P_i(T, V_{vert}) = P_i = k_1T\left(\frac{V_{vert}}{2} + \sqrt{\frac{T}{{k_2}^2} + \left(\frac{V_{vert}}{2}\right)^2}\right) \tag{11}$$

For a multi-rotor UAV, it is common to assume that the thrust generated is proportional to the angular speed squared [16], or $T_i = k_3{\omega_i}^2$ where, k_3 is a scaling factor converting from rotor angular speed ω to thrust T.

$$P_p(T, V_{air}) = c_2T^{\frac{3}{2}} + c_3(V_{air}cos\alpha)^2T^{\frac{1}{2}} \tag{12}$$

$$P_{par} = c_4{V_{air}}^3 \tag{13}$$

where, $k_2 = \sqrt{2\rho A}$
and

$$V_{air} = ||V_{air}|| = ||V_{ground} - V_{wind}|| \tag{14}$$

$$T = \sqrt{(mg - (c_5(V_{air}cos\alpha)^2 + c_6T))^2 + (c_4{V_{air}}^2)^2} \tag{15}$$

While hovering, $V_{vert} = 0$ and the induced power is reduced to

$$P_{i,hover}(T) = \frac{k_1}{k_2}T^{\frac{3}{2}} = c_1T^{\frac{3}{2}} \tag{16}$$

Therefore, $k_1, k_2, c_1, c_2, c_3, c_4, c_5$ are the parameters that are to be identified

Model Identification using experiments From equation eq(11) to eq(15), the power components are almost linear functions of payload and airspeed. To identify the unknown coefficients, three simple experiments are performed, namely hover, steady-state ascend/descend, and cyclic straight-line mission, on a UAV the power modeling of which we are interested in. In each experiment, the total power drawn is computed by multiplying voltage and current measurements from an onboard power module fitted in the UAV.

1. Experiment 1 - Hover - In this experiment, the UAV is loaded with different payloads and made to hover. The total power is given by equation eq(17) from which (c_1+c_2) can obtained . A least square fit of power with varying payload weight can also be derived.

$$P_{exp1} = P_{i,hover}(mg, 0) + P_p(mg, 0) = (c_1 + c_2)(mg)^{\frac{3}{2}} \tag{17}$$

2. Experiment 2 - Steady State ascend/descend - In this experiment, the UAV is commanded to ascend and descend at constant vertical speed between a defined altitude range without payloads. The total power is given by equation eq(18). Together with Experiment 1, there are four equations (hover, ascend, descend, and $c_1 = k_1/k_2$), and four unknown parameters (k_1, k_2, c_1, and c_2).

$$P_{exp2} = P_i(mg, V_{vert}) + P_p(mg, 0) \tag{18}$$

3. Experiment 3 - Cyclical straight lines - The goal of this experiment is to quantify the effect of parasite drag. The total power is given by equation eq(19), with the thrust T, and lift L and drag D defined by equation eq(8) and eq(9), respectively. The parameter c_3 is assumed to be 0 to simplify the identification process

$$P_{exp3} = P_i(T, 0) + P_p(T, V_{air}) + P_{par}(V_{air}) \tag{19}$$

$$= (c_1 + c_2)T^{\frac{3}{2}} + c_3(V_{air}cos\alpha)^2T^{\frac{1}{2}} + c_4V_{air}^3 \tag{20}$$

$$\simeq (c_1 + c_2)T^{\frac{3}{2}} + c_4V_{air}^3 \tag{21}$$

Based on the above experiments, the complete powewr consumption modeling of the UAV can be derived. As per the expermients conducted in [7] on an IRIS+ drone from 3D Robotics, the power consumption modeling shows a percentage devation of 10.7%, 2.2% and 16.5% in power during take-off, landing and steady state flight respectively.

2.2.2 Power Modeling Based on aerodynamic aspect

Raffaello D'Andrea in [9] provides a seminal contribution in modeling drone energy consumption by translating the fundamental flight principles of manned aircraft to a model for the much smaller scale of unmanned aerial drones. A power consumption model is obtained using an integrated approach that combines aerodynamic and drone design aspects into a single critical parameter: the lift-to-drag ratio r
The power consumed in kW can be approximated as

$$P = \frac{(m_p + m_v)v}{370\eta r} + p \tag{22}$$

where

- m_p : payload mass, in kg
- m_v : vehicle mass, in kg
- r : lift-to-drag ratio
- η : power transfer efficiency for motor and propeller
- p : power consumption of electronics, in kW
- v : cruising velocity, in km/h

The power consumed by such a formulation is a function of the total mass of the UAV and the velocity with which it flies. Using this simple formulation one can address the economics of flight very easily. The average energy cost per kilometer can be approximated by

$$\frac{c}{e}\left(\frac{(m_p + m_v)v}{370\eta r} + \frac{p}{v}\right) \tag{23}$$

where,

- c : cost of electricity in \$/kW.h
- e : charging efficiency

2.2.3 Power Modeling based on Helicopters

The power consumption equations for a multi-rotor UAV are obtained by extending the power consumption model that is available for single rotor helicopters [17].
In this formulation, an equation for the power consumed by a multirotor helicopter is derived in hover as a function of its weight. It is shown that the power it consumes is approximately linearly proportional to the weight of its battery and payload under practical assumptions. The power consumed by a multirotor drone is derived during hover, but not during flight, takeoff, or landing. In flight, the power consumed by the helicopter is often reduced due to translational lift [18], a phenomenon where air flowing horizontally along the rotor generates additional lift.
The average power during hover is consequently an upper bound on the average power during flight. We assume that the power consumed during takeoff and landing is, on average, approximately equivalent to the power consumed during hover.

Using [17], the power P^* is calculated in Watts for a single rotor helicopter in hover, with the thrust T in Newtons, fluid density of air ρ in kg/m^3, and the area ζ of the spinning blade disc in m^2 using

$$P^* = \frac{T^{\frac{3}{2}}}{\sqrt{2\rho\zeta}} \tag{24}$$

where the Thrust $T = (W + m)g$ and W is the frame weight in kg, m is the battery and payload weight in kg.
Usinh eq(24), the power for an n-rotor UAV is derived assuming that each rotor carries a

weight of $m' = m/n$ for batteries and payload and a frame weight of $W' = W/n$ meaning that the power is consumed by a single rotor. Therefore,

$$P' = (W' + m')^{\frac{3}{2}} \sqrt{\frac{g^3}{2\rho\zeta}} \tag{25}$$

So, the power consumed by all the n rotors is given by

$$P = nP' = (W + m)^{\frac{3}{2}} \sqrt{\frac{g^3}{2\rho\zeta n}} \tag{26}$$

Note : The inverse relationship between P and n seen in eq(26) is a result of n increasing the effective disc area of the propeller blades.
The linear approximation of the n-rotor UAV power consumption eq(26) can be expressed as

$$p(m) = \alpha m + \beta \tag{27}$$

where, α represents the power consumed per kilogram of battery and payload weight m and β is the power required to keep the quadopter frame in the air.

The authors in [8] have obtained (as shown in fig.2) that eq(26) closely fits eq(27) assuming a 3D Robotics ArduCopter Hexa-B hexacopter(as shown in fig.3) where $n = 6$, $\rho = 1.204\ kg/m^3$, $\zeta = 0.2\ m^2$, and $W = 1.5\ kg$. Applying a linear regression to eq(26) for $m = 0$–$3\ kg$ in increments of $0.001\ kg$ results in $\alpha = 46.7\ W/kg$ and $\beta = 26.9\ W$. The linear approximation eq(27) closely fits the exact equation eq(26), with a mean percent error of 3.1% and the largest difference being 6.3 W.

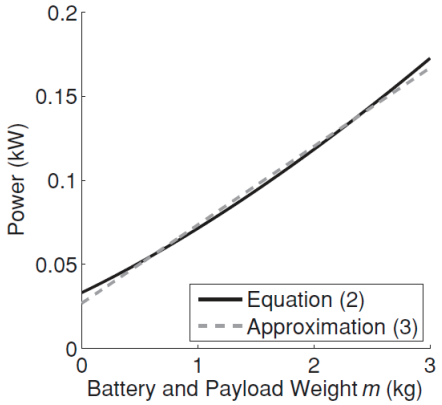

Figure 2: Linear approximation eq(26) fitted to the power consumption model eq(27)

Figure 3: a 3D Robotics ArduCopter Hexa-B hexacopter

2.2.4 Power Modeling using an extension of Helicopter

This power consumption modeling is based on the fact that UAVs expend energy to fight gravity and to counter drag forces due to forward motion and wind [13]. The UAV's control software adjusts the speed of each rotor to achieve the thrust and pitch necessary to stay aloft and travel forward at the desired velocity. The total required thrust by:

$$T = (m_{body} + m_{batt} + m_{package})g + F_{drag} \tag{28}$$

where m_{body}, m_{batt}, $m_{package}$ are the masses of the UAV body, battery and package(if present) respectively. F_{drag} is the total drag force acting on the UAV.
The pitch angle (α) for steady flight is calculated from

$$\alpha = tan^{-1}\left(\frac{F_{drag}}{(m_{body} + m_{batt} + m_{package})g}\right) \tag{29}$$

The drag force is estimated piecewise by the formulae

$$F_{drag} = \sum_i \frac{1}{2}\rho {v_a}^2 C_{Di} A_i \tag{30}$$

where,

- v : Velocity of the UAV
- v_a : Air speed
- ρ : Air density
- C_{Di} : Drag co-efficient of the i^{th} component
- A_i : Projected area of the i^{th} component

The drag coefficient for a quadrotor UAV is determined empirically using the drone's onboard pitch measurement while flying at various velocities

$$C_D = \frac{2m_{body} \times g \times tan(\alpha)}{\rho \times {v_a}^2 A_{body}} \tag{31}$$

The theoretical minimum power depends on the area swept by the rotors. In general, larger propellers are more efficient because the larger swept area allows them to achieve a given thrust at lower air velocity. However, they are less responsive because they have greater inertia. In addition, rotors must be spaced not to interfere with each other. These factors limit the rotor size.
For n rotors of diameter D, the theoritical minimum power to hover is [17]

$$P_{min,hover} = \frac{T^{\frac{3}{2}}}{\sqrt{\frac{1}{2}\pi n D^2 \rho}} \tag{32}$$

When the UAV moves at significant velocity or in significant wind, the minimum power requirement changes somewhat depending on the air speed and incident angle. The minimum power with forward motion can be calculated from conservation of momentum. Adapting from Hoffman et al. in [19], the power is given by:

$$P_{min} = T(vsin\alpha + v_i) \tag{33}$$

where v_i is the induced velocity required for a given thrust and can be found by the solution to the implicit equation

$$v_i = \frac{2T}{\pi n D^2 \rho \sqrt{(vcos\alpha)^2 + (vsin\alpha + v_i)^2}} \tag{34}$$

The theoretical minimum power is corrected by the overall power efficiency of the UAV, η, to get expended power:

$$P = P_{min}/\eta \tag{35}$$

η is determined empirically for the quadcopter model. Using eq(35), and the velocity of the UAV, we can easily calculate the power required per unit distance and the economics of the flight.

2.2.5 Power Modeling based on flight experiments using Regression

This is a class of modeling where the power consumption model of an UAV is designed emperically from field experiments. The UAV is subjected to various flight maneuvers and oprations and a power/energy expression is captured out of those maneuvers/operations using regression. The authors in [12] have derived a 9 variable power consumption model by performing various experiments on a commercial drone 3DR Solo.

To understand the factors that determine the energy consumption of a UAV, the following factors are considered for obtaining empirical data:

- Impact of Motion: The motions of a UAV can be divided into three types: hovering, horizontal moving and vertical moving. The energy consumption of each type of motion is studied.
- Impact of Weight: Typical UAVs carry payloads, such as camera equipment or parcels. The impact of different weights of payloads.

- Impact of Wind: The major environmental factor that affects the UAV profile is wind, including wind direction and speed. Wind may aid the energy consumption in some cases, as well as incurring resistance to the movement in other cases. We study the energy consumption of the test UAV in various wind conditions.

The experiments in [12] are described below

1. Impact of motion

   - Experiment 1: The test UAV hovers in the air without any movement in this experiment. The drone may slightly drift around the takeoff location due to deviation error of GPS modules. This experiment shows the baseline power consumption of a flying drone. From the recorded data, it is observed that the UAV can maintain a steady altitude with steady power consumption.
   - Experiment 2: The test UAV is made to ascend and descend continuously in a repeated fashion in this experiment. The barometer of the UAV shows the altitude data. Time series is used to compute the vertical acceleration and speed of the drone. Large power fluctuations are observed due to repeated vertical movements. It is also seen that the power consumption increases when the UAV ascends.
   - Experiment 3: The test UAV moves horizontally without altering its altitude in this experiment. The GPS data comprises of speed and course angle of the drone. The average wind speed and direction is also gathered using a wind speed meter during the experiment. Smaller power fluctuations are observed due to horizontal movements. We also observe the idle power consumption of the drone between the two experiments

   Fig. 4 depicts the recorded data traces of the three experiments.

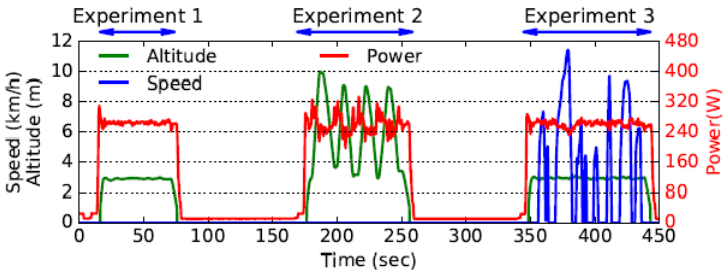

Figure 4: Motion and battery power consumption of the test drone.

2. Impact of weight
   Several experiments are carried out with different weights of payloads on the UAV to obtain empirical data. The drone is set to hover in the air without any movement to obtain the corresponding baseline power consumption as is seen in fig.5. It is seen that the power consumption increases with increasing payload

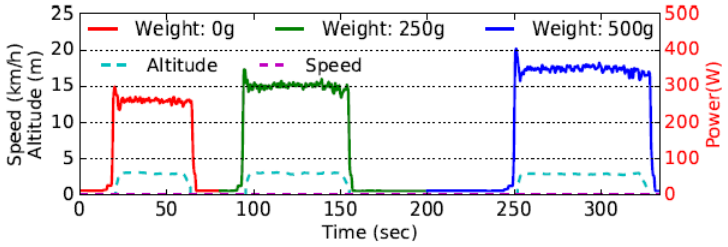

Figure 5: Battery power consumption of the test drone with different payload weights.

3. Impact of wind
   Several experiments under different wind conditions: headwind by flying against the direction of wind, and tailwind by flying along the direction of wind. The wind directions and average speeds are measured using a wind speed meter for each experiment. Once the wind direction is determined, the drone is set to fly into a headwind or tailwind at maximum speed (18 km/h). Fig.6 depicts the battery power consumption of the drone under different wind conditions. Smaller power consumption is observed when flying into headwind, which is due to the increasing thrust by translational lift.

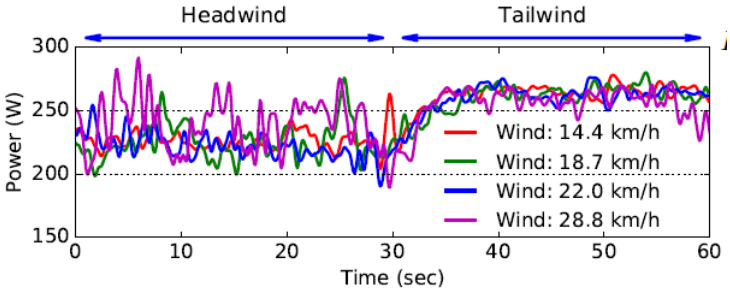

Figure 6: Battery power consumption of the test drone under different wind conditions.

Power Consumption Model using Regression A linear blackbox model of energy consumption for the UAV estimated by a number of measurement parameters is described by the following linear equation:

$$\tilde{P} = \begin{bmatrix} \beta_1 \\ \beta_2 \\ \beta_3 \end{bmatrix}^T \begin{bmatrix} ||\vec{v_{xy}}|| \\ ||\vec{a_{xy}}|| \\ ||\vec{v_{xy}}||||\vec{a_{xy}}|| \end{bmatrix} + \begin{bmatrix} \beta_4 \\ \beta_5 \\ \beta_6 \end{bmatrix}^T \begin{bmatrix} ||\vec{v_z}|| \\ ||\vec{a_z}|| \\ ||\vec{v_z}||||\vec{a_z}|| \end{bmatrix} + \begin{bmatrix} \beta_7 \\ \beta_8 \\ \beta_9 \end{bmatrix}^T \begin{bmatrix} m \\ ||\vec{v_{xy}}|| \\ ||\vec{w_{xy}}|| \\ 1 \end{bmatrix} \tag{36}$$

where

- $\vec{v_{xy}}$ and $\vec{a_{xy}}$ are the speed and acceleration vectors describing the horizontal movement of the UAV.
- $\vec{v_z}$ and $\vec{a_{xy}}$ are the speed and acceleration vectors describing the vertical movement of the drone.

- m is the weight of payload.
- $\vec{w_{xy}}$ is the vector of wind movement in the horizontal surface.
- $\beta_1, ...\beta_9$ are the coefficients and $||\vec{v}||$ denotes the magnitude of a vector.

$\beta_1, ...\beta_9$ is estimated by the standard regression method, if sufficient measurement data is collected. Assuming the uniform conditions (e.g. speed, wind) within a period of duration D, the total energy consumption of the drone is estimated by $\tilde{P}D$.

2.3 Research Gap

1. An UAV design combines the attributes of airplanes and helicopters. While airplanes are designed to travel long distances efficiently, helicopters are designed to hover efficiently [10]. In most cases, the power consumption modeling is derived from hovering action in Helicopters [14] as evident from the works done in [9], [13], [8], [11]. Some works like [13] have extrapolated the dynamics of hovering to capture the power consumption during leveled flight with constant velocity. An UAV operation involves stages of leveled flight, so deriving power from hovering and then extrapolating it for the entire flight can be a reason why the power consumption model cannot accurately capture the total power that is expended during an UAV operation.

2. There is a consideration where the power consumed during hover is an upper bound to the power consumed for other instances of the flight i.e take-off/landing/leveled translational motion etc [8]. This is based on the phenomenon of translational lift [18], a phenomenon that occurs when the UAV is in a horizontal motion and air flowing horizontally along the rotor generates additional lift. This intuition is not ideally true as the UAV is not at the same attitude for the entire duration of the flight and hence the rotors does not cross the air horizontally leveled at all instances. This consideration can be a reason for the inaccuracy in a power consumption model of an UAV.

3. In literature, none of the power consumption models that are designed analytically gives an optimum horizontal velocity that would minimize the power consumption for an UAV during leveled flight. The work done in [6] obtains the value of that airspeed intuitively and with rigorous flight tests. Moreover solution for an optimum vertical velocity during take-off/landing, and an optimum angle for ascend/desced can also be looked for. In literature, a standard angle for ascend/descend is considered as 45^o [10] but it is not verified if such an angle minimizes the power consumption.

4. Based on the literature surveyed, there is a wide variation in the power models with divergent power consumption values for essentially the same UAV operation. As seen in [6], the same UAV with the same operating settings shows wide variations in E_{pm}(Energy consumed per unit distance) values and range values with different power consumption models. These differences give a strong implication that we don't have an accurate or a benchmark power consumption model. The differences are because of different scopes and features of different models, different designs of

UAVs being modeled and different assumptions in operating conditions. Thus, current research has not reached a consensus on standards for UAV power consumption which is why existing models do not reflect UAV operations very accurately.

5. It is observed that different models use a different set of parameters for the power consumption modeling. Although different models are based on different philosophies but there is no metric to characterize the crucial parameters essential for power consumption modeling. For example model in [7] considers the effect of vertical velocity while the model in [13] does not consider the effect of vertical velocity whereas the model in [9] does not consider velocity at all. The discrepancies in power models maybe because of the lack of essential parameters in modeling. [7] considers a plethora of parameters initially but while deriving the power model, multiple parameters are lumped as a single variable which takes away the essence of considering multiple parameters at the first place.

6. None of the power consumption models that are derived from aerodynamic principles consider acceleration, either vertical or horizontal acceleration as a parameter for power consumption modeling. On the contrary, the UAV is subjected to changes in acceleration at various instants of the flight path like take-off/landing, undertaking turns etc. Such instances involve a change in velocity which introduces a change in acceleration. The velocity is considered static in most models due to a lack of means in obtaining the velocity in real-time [7] or due to oversimplification where leveled flights are considered as straight-line paths with constant velocities. In fact, some models do not consider the role of velocity at all [9].

2.4 Research Plan

2.4.1 Dynamic Power modeling using rotor speed

We are interested in deriving a power consumption model for an UAV. Using that model we wish to calculate the endurance (flight time or range) of that UAV and perform optimal path planning for a given operation. The power model should be applicable both online, where power will be calculated instantaneously as the UAV traverses with manual controls or offline, where given an objective, (say A to B problem in xyz plane with a predefined trajectory) one can use that model and estimate the energy that will be consumed when the UAV is subjected to travel.

We propose a dynamic power consumption model where given a flight path, one can estimate the power consumption profile for that path and integrate it to obtain the energy consumption. The model should also be able to calculate the additional power requirements in presence of external disturbances(say wind) when the UAV tries to maintain its flight path despite the disturbances.

- **Prelimenaries**

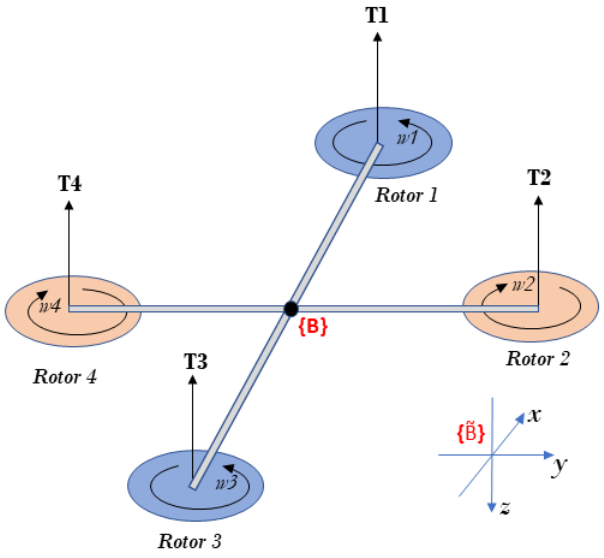

Figure 7: Quadrotor notation showing the four rotors, their thrust vectors and directions of rotation.

A quadrotor model is shown in fig 7. The body coordinate frame $\tilde{B}$ has its z-axis downward following the aerospace convention. The rotors consists of electric motors and are controlled by electronic speed controllers. The UAV generates thrust using these rotors which are fitted with propellers. The vertical component of this thrust which is known as lift balances the weight of the UAV while the horizontal component counteracts the drag and helps in translational motion. The parameters that affect thrust are :-
Fixed

1. No. of blades in a single propeller
2. Drag coefficient of blade
3. Blade chord length
4. Angle of attack of propeller blade
5. Propeller blade area

Variable

1. Drone Design
   (a) Drone weight (fixed with fixed battery)

(b) Payload weight

2. Environment
   (a) Wind velocity
   (b) Wind incident angle
   (c) Air density
   (d) Gravity

   Note - For wind(external disturbance), the UAV needs to lean against the wind with some roll, pitch and yaw angle depending upon the wind incident angle and prevent it from being deviated from its path/position. Some wind incident angle might also aid in translational motion.

3. Drone dynamics
   (a) Climb/Decend (Vertical motion) - All propellers produce same thrust. Climb/sink rate (vertical velocity) decides the required thrust profile.
   (b) Hover - All propellers produce same thrust.
   (c) Roll - Right side and left side propellers produce unequal thrust producing a rolling torque. Roll angle decides the required thrust in respective propellers.
   (d) Pitch - Front and rear propellers produce unequal thrust producig a pitching torque. Pitch angle decides the required thrust in respective propellers.
   (e) Yaw - Clockwise and counter-clockwise spinning propellers produce unequal torques resulting a yaw torque. Yaw angle decides the required thrust in respective propellers.
   (f) Cruise (Horizontal motion) - Combination of pitch and hover. The thrusts are unequal due to pitch. Due to pitch angle(θ_p) the vertical component of thrust is $Tcos(\theta_p)$ and as a result T required is higher than hover. Also, horizontal velocity depends on the pitch angle. See fig. 8

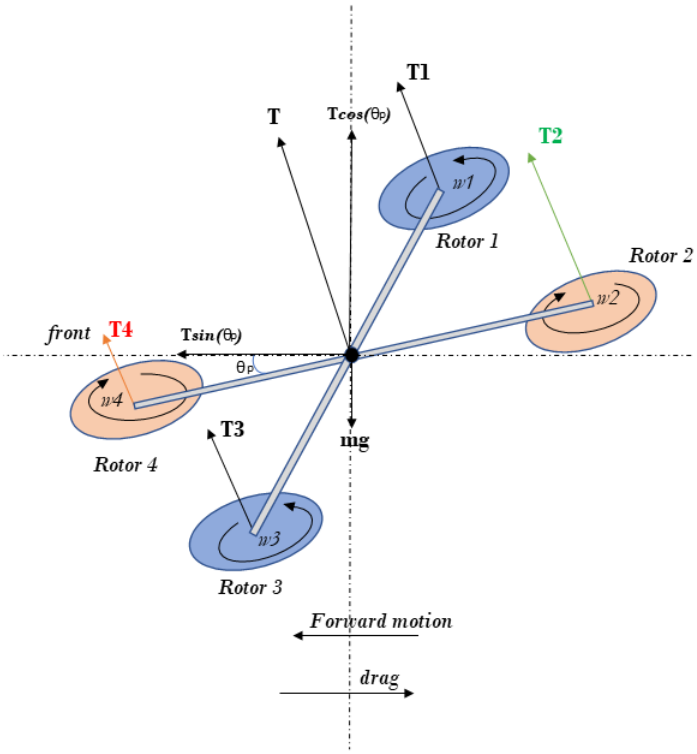

Figure 8: Horizontal motion of an UAV

In 3(c), 3(d) and 3(e) the total thrust produced by the propellers is constant and is equal to the gross weight of the UAV. In 3(f), $Tcos(\theta_p)$ is equal to the gross weight of the UAV.
$\underline{k}$ The phenomenon of Translational lift might lower T during cruise.

- **Drone dynamics with Thrust and angular velocity of rotors**
  Ideally,

$$\text{Thrust } T = bw^2 \tag{37}$$

where, w is the angular velocity in number of revolutions per minute(RPM) of the propeller/rotor and b depends upon the fixed parameters $1-5$ and 2(c).

The translational dynamics of the vehicle in world coordinates is given by Newton's second law

$$m\dot{v} = \begin{bmatrix} 0 \\ 0 \\ mg \end{bmatrix} - R_B^0 \begin{bmatrix} 0 \\ 0 \\ T \end{bmatrix} - Bv \tag{38}$$

where,

- v = velocity of the vehicle's center of mass in world reference frame
- m = total mass of the UAV
- B = aerodynamic friction
- R_B^0 = rotation matrix from vehicle frame to world coordinate frame

Pairwise differences in rotor thrusts cause the vehicle to rotate. The torque about the vehicle's x-axis, the rolling torque, is generated by the moments

$$\tau_x = d(T_4 - T_2) \tag{39}$$

where d is the distance from the rotor axis to the center of mass. We can write this in terms of rotor speeds by substituting eq(37)

$$\tau_x = db(w_4^2 - w_2^2) \tag{40}$$

Similarly, the torque about the vehicle's y-axis, the pitching torque, is given by

$$\tau_y = db(w_1^2 - w_3^2) \tag{41}$$

The torque applied to each propeller by the motor is opposed by aerodynamic drag given by

$$Q_i = cw_i^2 \text{ and } i \in \{1, 2, 3, 4\} \tag{42}$$

c depends on the same factors as b.
This torque exerts a reaction torque on the airframe which acts to rotate the airframe in the opposite direction to its rotation. The reaction torque about the z-axis is

$$\begin{aligned} \tau_z &= Q_1 - Q_2 + Q_3 - Q_4 \\ &= c(w_1^2 - w_2^2 + w_3^2 - w_4^2) \end{aligned} \tag{43}$$

So, a yaw torque is generated simply by appropriate coordinated control of all four rotor speeds.
The total torque applied to the airframe according to eq(40), eq(41) and eq(43) is $\tau = (\tau_x, \tau_y, \tau_z)^T$.
The rotational acceleration is given by Euler's equation of motion

$$J\dot{w} = -w \times Jw + \tau \tag{44}$$

where J is the 3×3 inertia matrix of the UAV and w is the angular velocity vector. The motion of the quadrotor is obtained by integrating the forward dynamics equations eq(38) and eq(44) where the forces and moments on the airframe are functions of rotor speeds.

$$\begin{bmatrix} T \\ \tau \end{bmatrix} = \begin{bmatrix} -b & -b & -b & -b \\ 0 & -db & 0 & -db \\ db & 0 & -db & 0 \\ c & -c & c & -c \end{bmatrix} \begin{bmatrix} w_1^2 \\ w_2^2 \\ w_3^2 \\ w_4^2 \end{bmatrix} = A \begin{bmatrix} w_1^2 \\ w_2^2 \\ w_3^2 \\ w_4^2 \end{bmatrix} \tag{45}$$

The matrix A is constant and full rank if $b, c, d > 0$ and we can obtain the required rotor speeds as

$$\begin{bmatrix} w_1^2 \\ w_2^2 \\ w_3^2 \\ w_4^2 \end{bmatrix} = A^{-1} \begin{bmatrix} T \\ \tau_x \\ \tau_y \\ \tau_z \end{bmatrix} \tag{46}$$

- **Control architecture for translating forward flight to rotor speeds**
  Here, a PID control architecture is used to describe the control scheme on the UAV for translational motion. This architecture is based on the work done by Peter Corke[16]
  Altitude is controlled by a proportional-derivative controller

$$T_z = K_p(z^* - z^\#) + K_d(\dot{z}^* - \dot{z}^\#) + T_0 \tag{47}$$

  $T_0 = mg$ is the weight of the vehicle. z^* and $z^\#$ are the desired and actual altitudes respectively. eq(37) and eq(47) determine the average rotor speed.
  For pitch and x-translational motion, a proportional and derivative controller to compute the required pitching torque on the airframe based on the error between desired and actual pitch angle

$$\tau_y^* = K_{\tau,p}(\theta_p^* - \theta_p^\#) + K_{\tau,d}(\dot{\theta_p}^* - \dot{\theta_p}^\#) \tag{48}$$

  where, $K_{\tau,p}$ and $K_{\tau,d}$ are controller gains, θ_p^* and $\theta_p^\#$ are the desired and actual pitch angles respectively.
  Consider a coordinate frame $\tilde{B}$ attached to the vehicle and with the same origin as B but with its x and y axes in the horizontal plane and parallel to the ground. The thrust vector is parallel to the z-axis of frame B and pitching the nose down, rotating about the y-axis by θ_p, generates a force

$${}^{\tilde{B}}f = \mathscr{R}_y(\theta_p).\begin{bmatrix}0\\0\\T\end{bmatrix} = \begin{bmatrix}Tsin(\theta_p)\\0\\Tcos(\theta_p)\end{bmatrix}$$

  The component ${}^{\tilde{B}}f_x$ accelerates the vehicle in the ${}^{\tilde{B}}x$-direction, and we have assumed that θ_p is small.

$${}^{\tilde{B}}f_x = Tsin(\theta_p) \approx T\theta_p \tag{49}$$

  We can control the velocity in this direction with a proportional control law

$${}^{\tilde{B}}f_x{}^* = m \times K_f({}^{\tilde{B}}v_x{}^* - {}^{\tilde{B}}v_x{}^\#) \tag{50}$$

  where K_f is the controller gain, ${}^{\tilde{B}}v_x{}^*$, ${}^{\tilde{B}}v_x{}^\#$ are the desired and actual velocities in world reference frame obtained from ${}^{B}v_x$ which is in body frame estimated by an inertial navigation system.
  Combining eq(49) and eq(50), we obtain the desired pitch angle required to achieve the desired forward velocity.

$$\theta_p^* \approx \frac{m}{T}K_f({}^{\tilde{B}}v_x{}^* - {}^{\tilde{B}}v_x{}^\#) \tag{51}$$

  Using eq(48) we compute the required pitching torque, and then using eq(46) the required rotor speeds.
  If the position of the vehicle in the xy-plane of the world frame is $p \in \mathbb{R}^2$ then the desired velocity is given by the proportional control law based on the error between the desired and actual position.

$${}^0v^* = K_p({}^0p^* - {}^0p^\#) \tag{52}$$

The desired velocity in the xy-plane of $\tilde{B}$ is

$$^{\tilde{B}}v = {}^{0}\mathscr{R}_{\tilde{B}}(\theta_y).{}^{0}v,\ \mathscr{R} \in \mathrm{SO}(2) \tag{53}$$

which is a function of yaw angle θ_y

$$\begin{bmatrix} {}^{\tilde{B}}v_x \\ {}^{\tilde{B}}v_y \end{bmatrix} = \begin{bmatrix} cos(\theta_y) & -sin(\theta_y) \\ sin(\theta_y) & cos(\theta_y) \end{bmatrix} \begin{bmatrix} v_x \\ v_y \end{bmatrix} \tag{54}$$

To summarize, we have the desired position of the quadrotor in world coordinates. The position error is rotated from the world frame to the body frame and becomes the desired velocity. The velocity controller implements eq(51) and its equivalent (if position of the vehicle is in the xy plane) for the roll axis and outputs the desired pitch and roll angles of the quadrotor. The attitude controller is a proportional-derivative controller that determines the appropriate pitch and roll torques to achieve these angles based on feedback of current attitude and attitude rate. The yaw control block determines the error in heading angle and implements a proportional-derivative controller to compute the required yaw torque. Then from these three torques and T_z as calculated abouve, we can obtain the required rotor speeds using eq(46). If instead of desired position we have a given trajectory which the UAV is supposed to follow, we can formulate the trajectory as a sequence of coordinates and apply the above philosophy to derive the required roll, pitch, yaw torque and thrust dynamics with respect to time. From that we derive the rotor speed profiles.

- **Power Calculation**
  The shaft power for a DC motor drive is given by

$$P = \frac{2\pi \times w \times T_{or}}{60} \tag{55}$$

where w is the angular speed of the motor in RPM and T_{or} is the torque in $N-m$. Power P is in Watts. According to Disk actuator theory[14], the torque produced by a rotor is given by

$$T_{or} = \frac{1}{2} T_q \rho A w^2 R^3 \tag{56}$$

where T_q is the torque coefficient which is fixed for a given propeller.ρ is air density, A is propeller disk area and R is blade chord length.

From eq(55) and eq(56), $P \propto w^3$. Here ρ is assumed constant for an operation while remaining parameters are constant by mechanical construction of the UAV. So, we map every dynamics and every parameter that affects thrust to a single variable for obtaining the power consumption profile of an UAV.

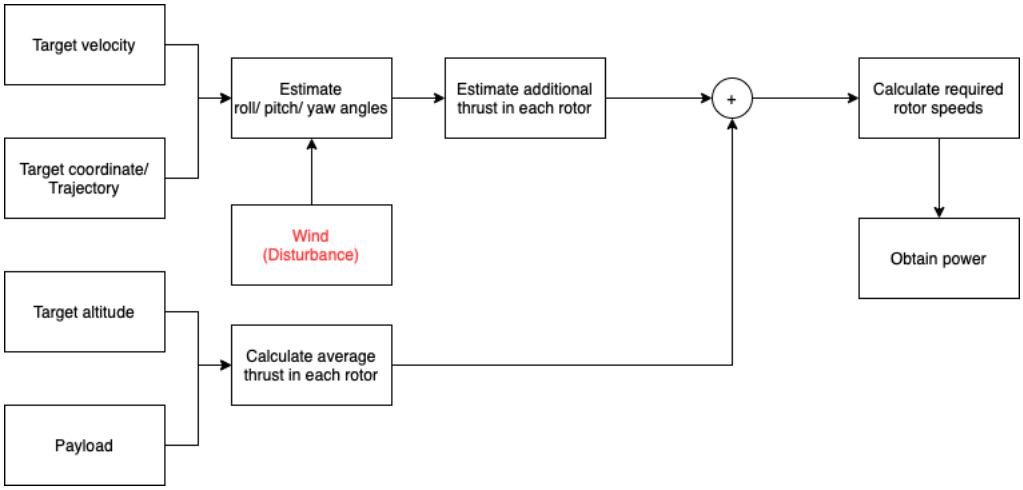

Figure 9: Snapshot of the power calculation philosophy

In an ideal case, with a given trajectory or hover action, we can plan the set of manuevers (3(a) to 3(f)) that will be required to execute that trajectory and obtain the thrust profiles that will be required in the propellers. From the thrust profiles, we can obtain the w(RPM) profiles and calculate the dynamic power that will be consumed by each propeller. Using battery efficiency and charging efficiency we can estimate the power that will be consumed in an operation.

For a non-ideal situation with wind at play, we plan to employ a sensing mechanism as shown in fig 10 (R_1, R_2, R_3, R_4) represents the sensing regions). Such sensors will be able to detect wind velocity and wind incident angle on the UAV body. Based on the applicable wind, we can obtain the required thrust to counteract that wind. From that thrust comes the required estimates of roll, pitch and yaw angle and from these estimates, we can obtain the w(RPM) profiles and then derive the dynamic power that will be applicable in counterating wind.

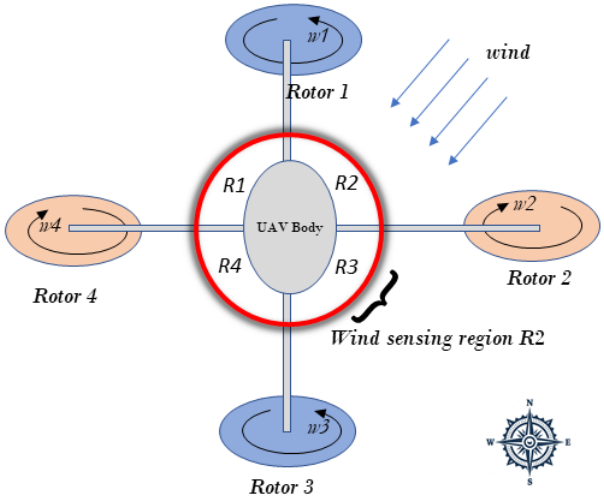

Figure 10: An UAV faced by wind from North East

- Simulations using MATLAB
  Based on the above philosophy, we perform simulations of an UAV motion using MATLAB. We give commands to a UAV in terms of cartesian coordinates and then obtain the angular speeds of all four rotors. The simulations are performed using a quadcopter model avaiabe in the Robotics Toolbox (RTB10.x) of MATLAB R2021a. This toolbox is designed by Peter Corke. The experiments were carried out on an Intel Core i5 computer at 3.50 GHz with 8 GB RAM using Windows 10 operating system.

  Here, the UAV is given coordinates as commands in the Cartesian cooordinate system. The UAV is initially at (0,0,0). w(RPM) with respect to time is plotted for all four rotors.

  - **Simulation 1 :**
    Initial position = (0,0,0), Target Position = (0,0,2)
    Simulation time = 5 seconds.
    The RPM profiles are shown in fig.11

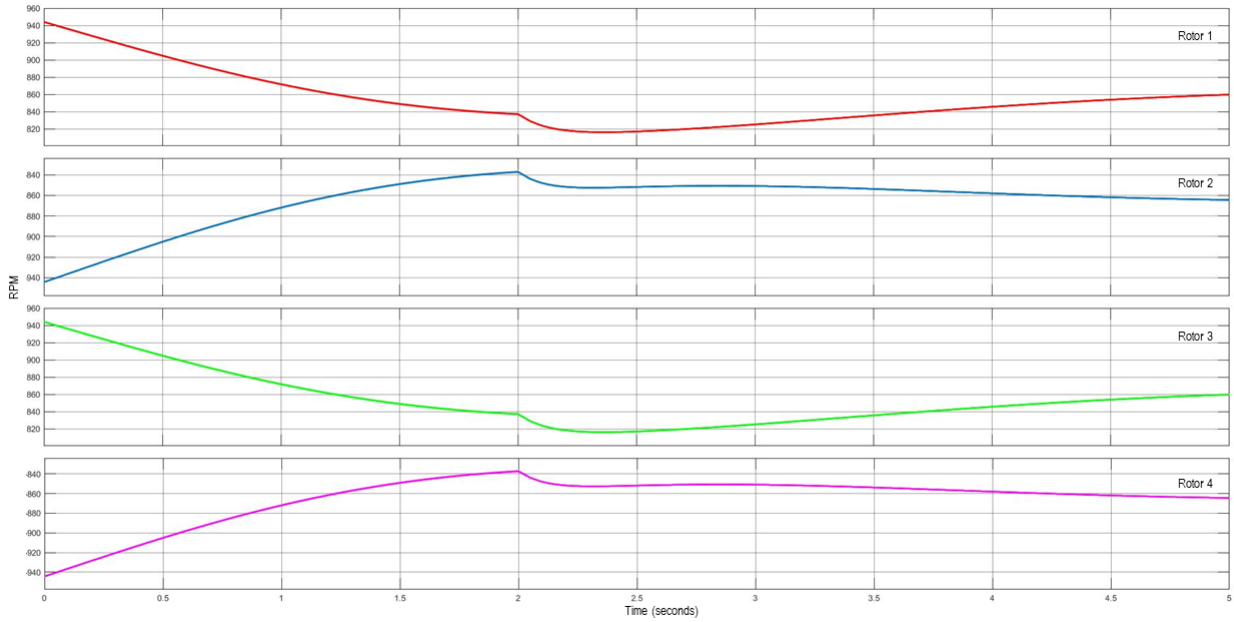

Figure 11: Simulation 1

– **Simulation 2 :**
Initial position = (0,0,0), Target Position = (4,0,2)
Simulation time = 5 seconds
The RPM profiles are shown in fig.12

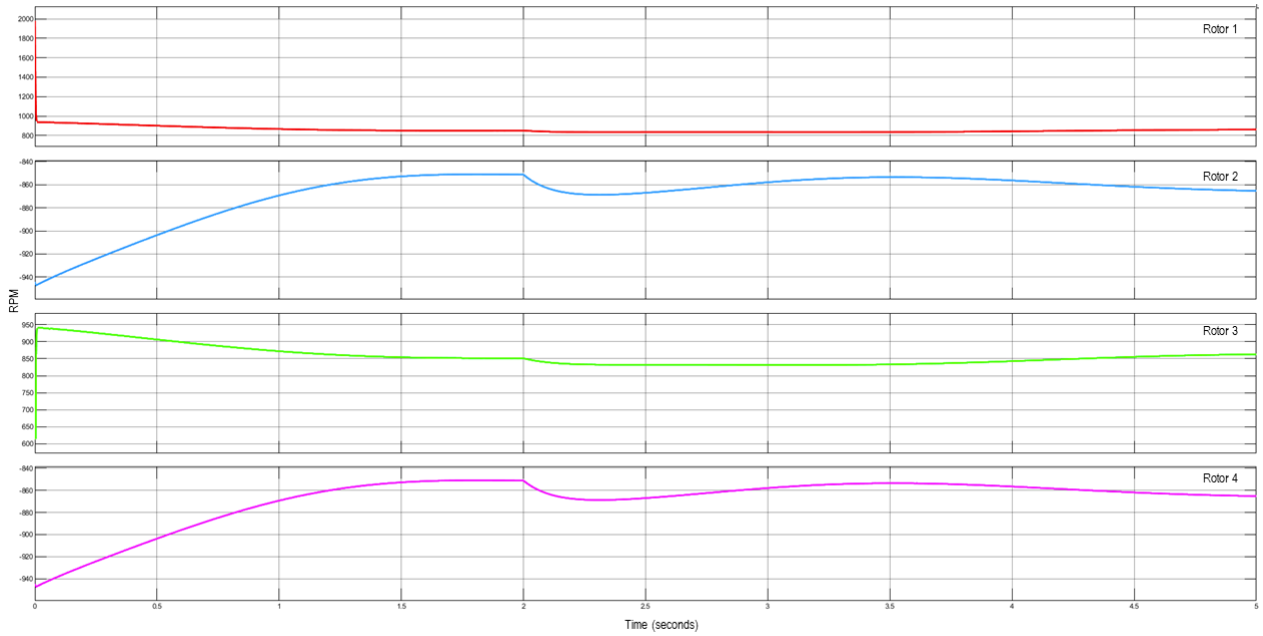

Figure 12: Simulation 2

– **Simulation 3 :**

Initial position = (0,0,0), Target Position = (4,4,2)
Simulation time = 5 seconds
The RPM profiles are shown in fig.13

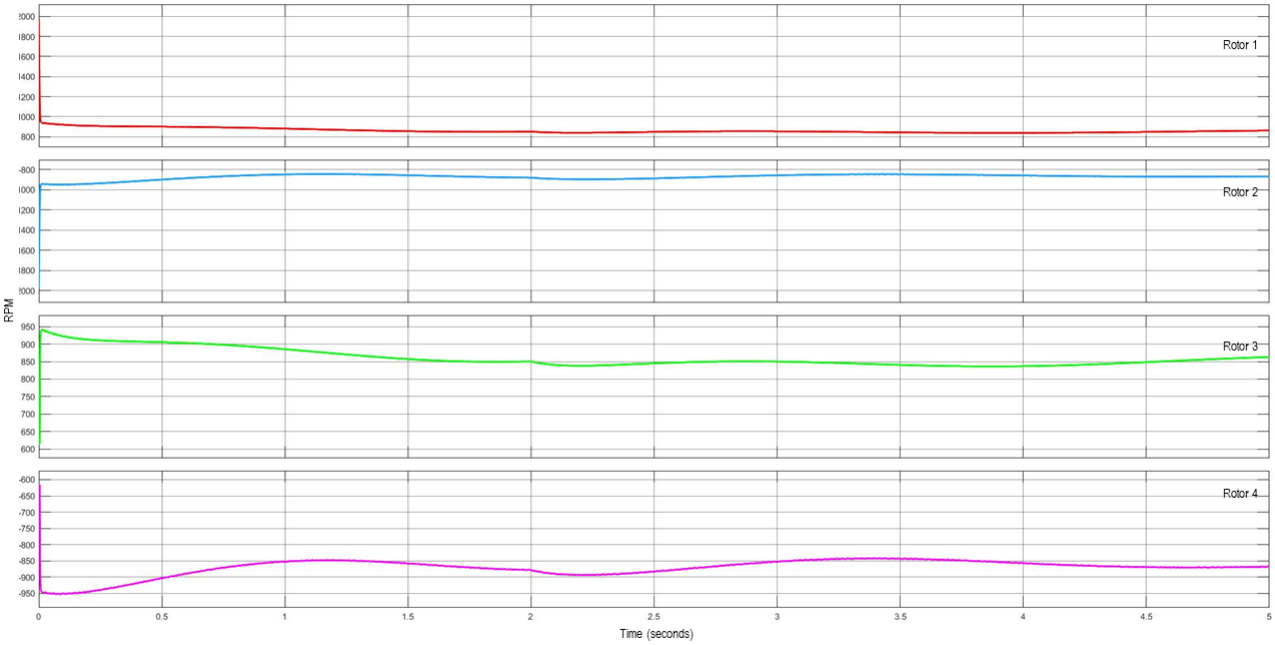

Figure 13: Simulation 3

– **Simulation 4 :**
Initial position = (0,0,0), Target Position = (0,0,1) at time $t = 0$s, (0,0,2) at time $t = 5$s, (0,0,3) at time $t = 10$s
Simulation time = 20 seconds
The RPM profiles are shown in fig.14

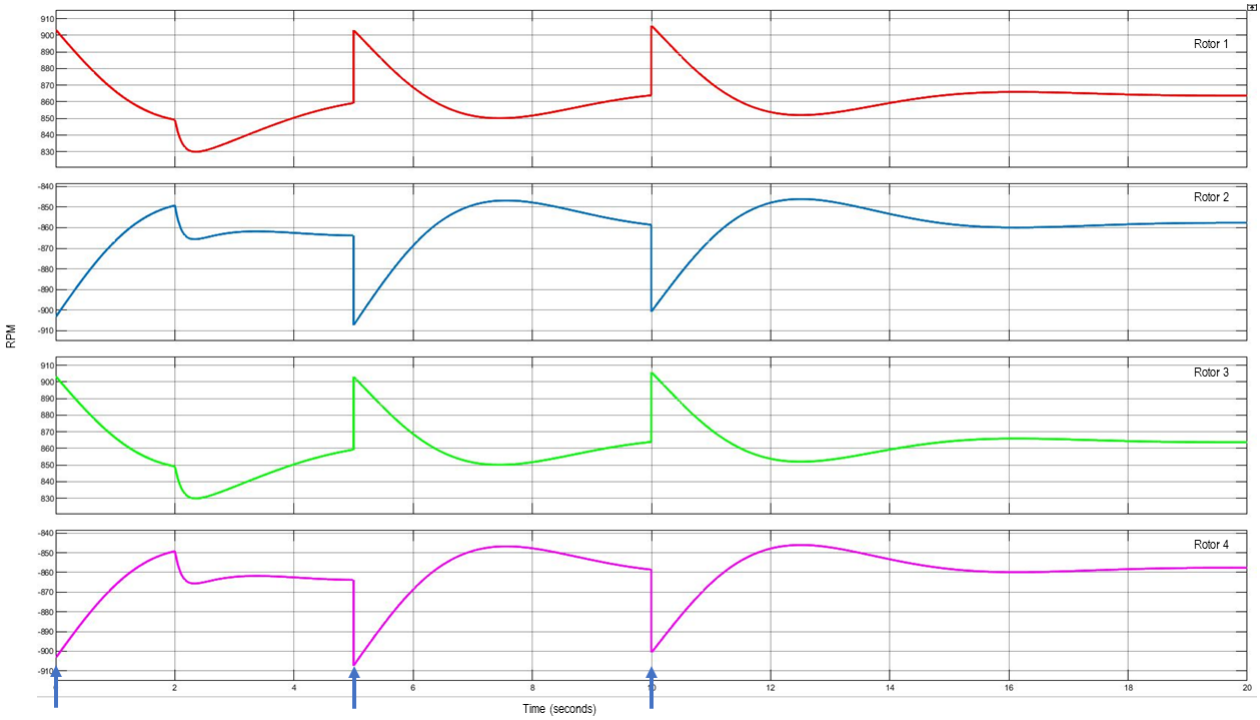

Figure 14: Simulation 4

- Inference - As seen from above figures, the angular speeds of the rotors show substantial variations when they are commanded for various coordinates. Using these profiles we intend to compute the dynamic power. The results from simulations need to be validated against a physical setup where we intend to calculate the practical power from voltage and current measurments of the rotors.

3 Path Planning

3.1 What is path planning

Path planning refers to the generation of a set of waypoints between an initial location and a desired destination with an optimal or near-optimal performance under specific constraint conditions. Path planning is performed to ensure the following attributes [20] :

- Stealth: Stealth means safety. The topography of an area through which the UAV travels may include buildings, mountains, forest cover etc, so it is essential that it doesnot crash against any such objects. Moreover, in military applications, UAVs have to ensure that they stay away from the realm of enemy radars or evade when there is a pursuit by an enemy UAV.
- Physical Feasibility: The physical feasibility of a route refers to the physical limitations from the use of UAVs. They include the following constraints.
  - Flying time
  - Payload weight
  - Communication range
  - Maximum translational velocity
  - Maximum climb/sink rate
  - On-board computational power
- Performance of Mission: Each flight has its special mission. This depends on the application. For example in applications like emergency responsiveness, the operator would want to reduce the time of operation while in parcel delivery, the operator would like to reduce the cost of operation. Certain missions require multiple trips by the same UAV to improve the efficiency of operation.
- Cooperation: The path planning algorithm must be compatible with the cooperative nature envisioned for the use of UAVs. A flight mission might involve multiple UAVs and in such an applications, the ability to coordinate with the routes flown by other UAVs become vital for a smooth and efficient operation.
- Real-Time Implementation: The flight environments of the UAVs are usually constantly changing. Therefore, the route-planning algorithm must be able to adapt to those changes and at the same time be computationally efficient.

3.2 Literature Review on path planning

The main objective of UAV path planning is to design flight paths with minimum comprehensive costs and maximum safety. The major dimensions of UAV path planning in literature are based on aspects of algorithm (deterministic/non-deterministic), time-domain (online/offline), and space domain (2D/3D)

- Dorling et. al in [8] have solved Vehicle Routing Problems as Multi-trip Vehicle Routing Problem (MTVRP) while considering battery and payload weight as parameters in the energy consumption modeling that governs the cost of a trip. Two

MTVRPs are solved, one that minimizes the time of an operation given a budget and other that minimizes the cost of an operation given a time limit. The authors have derived their own energy consumption model and claimed that the energy consumed is irrespective of whether the drone is hovering or flying with constant velocity. They have also concluded that energy consumption varies linearly with weight. The authors have derived MILPs for the VRP and have also used SA approach to obtain suboptimal solutions when the region of application is very large. Given an operation, solutions to the VRP are the number of UAVs, the routes they fly, battery weight and payload weight. It is shown that minimum time has an inverse exponential relationship with minimum cost.

- Authors of [21] solve a multi-modal path planning problem for UAVs under a low altitude dynamic urban environment. A Multi-objective path planning (MOPP) framework concerning travel time and safety level has been proposed. To this end, a static SIM is offline established to indicate the main static obstacles in the geography map, and a dynamic SIM is online constructed to capture unexpected obstacles that are not available in the geography map during flying. Then a joint offline and online search method has been developed to address the MOPP problem. The performance of the MOPP is evaluated using metrics consisting of the average and maximum runtime of the program, the UAV trajectory, travel time, and the total safety index. A travel time and safety index tradeoff curve is provided which can provide the users to select a Pareto optimal path according to their preferences. The perception range used for dynamic SIM decides the travel time in case of online replanning but that is restricted to the sensing infrastructure that is available during practical implementation.

- A Multi-Step A*(MSA*) search algorithm is proposed in [22] for four-dimensional multi-objective path panning of an UAV in a large dynamic environment. Generally, the path planning algorithms outputs a sequence of linear tracks in any grid-based motion planning scheme where track angle and velocity are restricted by assumptions. Here in this work, MSA* employs a variable successor operator and finds a cost-optimal path using variable length, angle and velocity trajectory segments. The multiple objectives addressed are safety, flying rules, delivery time and fuel consumption. The constraints considered in flight are cruise velocity, altitude, rate of climb, turn radius, vehicle separation, storm cell avoidance and population risk criterion. It is concluded that, on average, the computational time of MSA* is four times better than A* while the total cost is only marginally improved. It has been also shown that MSA* is suitable for online replanning as the average computation time is a fraction of the minimum track traversal time.

- Roberge et. al in [23] have used and compared two evolutionary algorithms for solving the real-time path planning problem of an UAV in a complex 3D environment. They have proposed a comprehensive cost function that includes optimal criteria like the length of the path, altitude and danger zones and feasible criteria like power availability, and collision avoidance. The cost function can easily be integrated with any other non-deterministic algorithm. They have concluded that GA produces superior path planning results than PSO. Later they have developed a parallel computing paradigm between these two algorithms in a single program and improved its execution time. It is classified as a multiple-deme parallel GA

where sub-populations evolve independently while allowing some level of migration between the demes.

- Sundar and Rathinam in [24] have proposed an algorithm for obtaining a sequence of routes for an UAV in the presence of multiple refueling depots. The task of the UAV is to visit a set of target points ideally for a surveillance application in a region with the flexibility of using multiple refueling stations such that the overall fuel consumption by the UAV is minimized. The UAV in this context is modeled as a Dubins' vehicle with a minimum turning radius and an optimal heading is considered at each target location. This combinatorial difficulty is handled using an approximation algorithm with some added heuristic layers and it is seen that solutions with costs within 1.4% of the optimum are obtained relatively quickly. It is also shown that when heuristics are added, the average deviation of the sub-optimality of feasible solutions are comparatively lower as the number of targets increase.

We have collatd the results and have elaborated on types of path planning in the following section.

3.3 Types of path planning

3.3.1 Offline path planning

Offline path planning is also known as global path planning. Under this situation, the environment is static, and its global information is known a priori in the control design. This approach is expensive in implementation and relatively well studied in the existing literature [25].

Offline path planning scenerio The following offline path planning scenerio is based on [8]

Problem Statement Given a geographical region with locations having specific demands, a set of UAVs needs to be deployed to fulfil those demands with certain objectives. The UAVs depart from a central depot which also act as a charging/battery swapping station and an UAV can be reused for multiple trips to increase the efficiency of the operation.

Objectives

1. Minimize the time of operation given a budget B (Emergency responsiveness)
2. Minimize the cost of operation given a time T (Parcel delivery logistics)

Solution Here a Path Planning Algorithm (PPA) is employed for this Path Planning Problem (PPP) which will satisfy the above objectives given a set of constraints (as discussed below) and obtain optimal/quasi-optimal routes for an effective operation. The solution to this PPP is in the form of the number of UAVs required, the routes that they fly and the battery capacity required for each route.

Path A path is defined as a route that starts and ends at the depot. The illustration given in figure 15 depicts two UAVs flying three routes. Whilst UAV 2 flies a single route, visiting locations 4–7, UAV 1 flies two routes. During its first route, UAV 1 visits locations 1–3, then returns to the depot to swap batteries and pick up more packages. After the swap, it flies its second route, visiting locations 8–10.

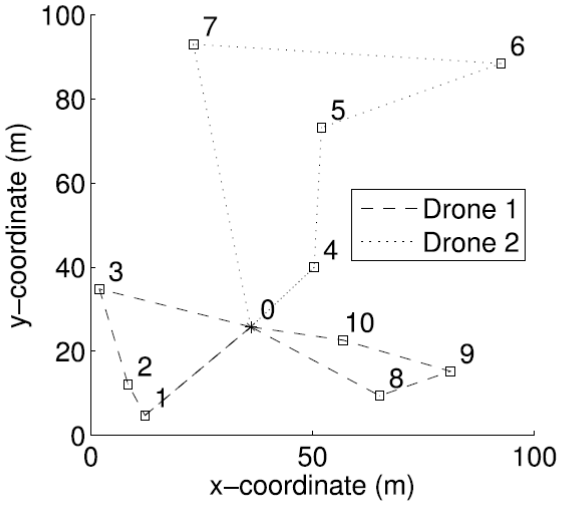

Figure 15: Example showing two flying three routes

The path planning algorithm optimize the routes flown by a set of UAVs in order to visit the set of locations N. Location 0 is the depot. Each location $i \in N_0$, where the set $N_0 = N \backslash 0$, has a demand D_i which represents the weight of the package in kg that will be delivered to location i. Every location, except for the depot, is visited only once by an UAV, and τ s is spent at each location to descend, deliver the package, and ascend.

Assumptions

- UAVs fly between locations with constant velocity
- Impact of weather on flight is neglected
- Demand in each location can be fully satisfied by a single UAV
- No recharging during trips
- There exists a single depot
- There exist battery packs with different capacities

Energy Consumption Model A energy consumption model has to be chosen such that energy consumed by an UAV during a trip can be captured as a function of battery and payload weight

Decision variables and constraints This section discusses the decision variables, constants, and constraints that are applicable in this PPP. The constraints can be put into categories related to limiting each UAV's route, reusability, timing, energy consumption, capacity, as well as the total cost of making deliveries. Decision variables and constants are described below their corresponding constraints. It is ensured that every route is valid through

$$\sum_{\substack{j \in N \\ j \neq i}} x_{ij} = 1 \qquad \forall i \in N_0 \tag{57}$$

$$\sum_{\substack{j \in N \\ j \neq i}} x_{ij} - \sum_{\substack{j \in N \\ j \neq i}} x_{ji} = 0 \qquad \forall i \in N_0 \tag{58}$$

To create a routing map for the UAVs, the edge variables x_{ij} is used, where $x_{ij} = 1$ if the UAV moves from location i to j, and $x_{ij} = 0$ otherwise. Constraint eq(57) guarantees that every location, except for the depot, is visited exactly once by an UAV, while eq(58) ensures that an UAV arriving at location i also departs from location i.

The reusability constraints

$$\sum_{j \in N_0} \sigma_{ij} \leq x_{i0} \qquad \forall i \in N_0 \tag{59}$$

$$\sum_{j \in N_0} \sigma_{ji} \leq x_{0i} \qquad \forall i \in N_0 \tag{60}$$

$$\sum_{j \in N_0} x_{0i} - \sum_{(i,j) \in N_0 X N_0} \sigma_{ij} \leq M \tag{61}$$

determine whether or not an UAV can be reused after returning to the depot. The reuse decision variable is σ_{ij}, where $\sigma_{ij} = 1$ if the UAV leaves location i for the depot, gains a fresh battery and set of packages, then flies to location j to begin a new route; otherwise $\sigma_{ij} = 0$. Constraint eq(59) implies that if an UAV returns to the depot from location i, it is available for use again to fly to another location. Constraint eq(60) ensures that if a reused UAV leaves from the depot to location i, it arrived previously from another location. The number of UAVs that can be purchased, and can therefore fly simultaneously, is limited to M by eq(61).

Applying demand constraints

$$\sum_{j \in N} y_{ji} - \sum_{j \in N} y_{ij} = D_i \qquad \forall i \in N_0 \quad and \quad i \neq j \tag{62}$$

$$y_{ij} \leq K x_{ij} \quad \forall (i,j) \in NXN, i \neq j \tag{63}$$

to ensure that each location receives what it demands. The payload weight between locations i and j is represented by the decision variable y_{ij} in kg. The constant K is a large value representing an upper bound for constraints. Constraint eq(62) makes sure that the payload weight when leaving location i is D_i kg less than upon arrival. Constraint eq(63) sets the payload weight of each edge without a vehicle to 0 kg.

Enforce timing is calculated through

$$t_i - t_j + \tau + d_{ij}/v \leq K(1 - x_{ij}) \qquad \forall (i,j) \in NXN_0 \quad and \quad i \neq j \tag{64}$$
$$t_i - a_i + \tau + d_{i0}/v \leq K(1 - x_{i0}) \qquad \forall i \in N_0 \tag{65}$$
$$a_i - t_j + \tau + d_{0j}/v \leq K(1 - \sigma_{ij}) \qquad \forall (i,j) \in N_0XN_0 \quad and \quad i \neq j \tag{66}$$
$$t_i \leq l \forall i \in N_0 \tag{67}$$
$$l \leq T \tag{68}$$

A location $i \in N_0$ is visited by an UAV at time t_i in seconds. The time in seconds that an UAV returns to the depot directly after leaving location i is a_i. Note that $a_i = 0$ if $x_{i0} = 0$, and $a_i > 0$ otherwise. The overall delivery time l is the time in seconds when all UAVs have completed their deliveries. Constant values related to timing include the speed v in m/s of the UAVs in the air, the distance d_{ij} in m between locations i and j, as well as the time τ in seconds spent at each location descending, delivering a package, and ascending. UAVs must complete their deliveries by the delivery time limit T in seconds. Constraint eq(64) keeps track of the time t_i that each location i is visited by an UAV. Similarly, eq(65) keeps track of the time a_i that an UAV arrives at the depot from location i. Constraint eq(66) ensures that times are correct for UAVs that are reused after returning to the depot. The overall delivery time l is set by eq(67), and the delivery time limit T is guaranteed by eq(68).

Carrying capacity is restricted through

$$q_{ij} + y_{ij} \leq Qx_{ij} \qquad (i,j) \in NXN \quad and \quad i \neq j \tag{69}$$
$$z_i/\zeta - \zeta_i \leq K(1 - x_{i0}) \qquad \forall i \in N_0 \tag{70}$$
$$\zeta_i - \zeta_j \leq K(1 - x_{ji}) \forall (i,j) \in N_0XN_0 \quad and \quad i \neq j \tag{71}$$
$$q_{ij} \geq \zeta_j - K(1 - x_{ij}) \forall (i,j) \in N_0XN_0 \quad and \quad i \neq j \tag{72}$$
$$q_{i0} \geq \zeta_i - K(1 - x_{i0}) \quad \forall i \in N_0 \tag{73}$$

The battery weight between locations i and j is represented by the decision variable q_{ij} in kg. To assist with optimizing the battery weight, the decision variable ζ_i tracks the battery weight in kg at location i. The energy consumed from an UAV's battery by the time it arrives at the depot directly after leaving location i is z_i kJ. Note that $z_i = 0$ if $x_{i0} = 0$, while $z_i > 0$ otherwise. The constant ζ is the energy density of the battery in kJ/kg. The capacity of the UAV between locations i and j is restricted to Q kg by eq(69). The weight ζ_i of the battery at each location i is set by eq(70) and eq(71): constraint eq(70) finds ζ_i for the locations visited just before the depot, while eq(71) sets $\zeta_i = \zeta_j$ if the UAV flies directly from location i to location j. The weight q_{ij} of the battery between locations i and j is required by eq(69) and is found through constraints eq(72) and eq(73). Constraint eq(72) sets $q_{ij} \geq \zeta_j$ if the UAV flies between locations i and j, while eq(73) sets $q_{i0} \geq \zeta_i$ if the UAV flies from location i to the depot.

Energy restrictions are enforced by

$$f_i - f_j + p(m_{ij})(d_{ij}/v + \tau) \leq K(1 - x_{ij}) \qquad \forall (i,j) \in NXN_0 \quad and \quad i \neq j \tag{74}$$
$$f_i - z_i + p(m_{i0})(d_{i0}/v + \tau) \leq K(1 - x_{i0}) \qquad \forall i \in N_0 \quad and \quad i \neq j \tag{75}$$
$$z_i \leq Kx_{i0} \tag{76}$$

The decision variable f_i represents the energy in kJ consumed from an UAV's current battery upon reaching location $i \in N_0$. The power $p(m)$ in kW consumed by an UAV with a battery and payload weight of m kg is estimated from the power consumption model. The weight in kg of the UAV's battery and payload between locations i and j is $m_{ij} = q_{ij} + y_{ij}$. Constraint eq(74) forces f_i to equal the total energy consumed along the route up to location i. Constraint eq(75) makes z_i equal to the energy consumed flying the entire route that ends at location i. To ensure that $z_i = 0$ if the UAV does not fly from location i to the depot, and that $z_i > 0$ otherwise, eq(76) is included. Note that constraints eq(74) and eq(75) are linear because the power $p(m_{ij})$ is a linear approximation.

Costs are kept in line with the budget B through

$$c = F \sum_{i \in N_0} x_{0i} - F \sum_{(i,j) \in N_0 X N_0} \sigma_{ij} + \epsilon \sum_{i \in N_0} z_i \tag{77}$$

$$c \leq B \tag{78}$$

The cost of an UAV is F financial units, while the budget is limited to B financial units. The constant ϵ is the cost in financial units of a kJ of energy. Constraint eq(77) calculates the total cost c of performing the deliveries. The leftmost term of eq(77) represents the cost of UAVs assuming that each route requires a new UAV, while the second term represents the savings provided by reusing UAVs; together they equal the total cost of UAVs. The rightmost term is the cost of energy. The total cost is restricted to the budget by eq(78). The constraints in this section assume each UAV's battery is sized to provide exactly enough energy for the upcoming route. The constraints can, however, be adjusted to find the optimum combination of discrete battery sizes. Assume a set of battery types $\tilde{B}$ exists, where each battery type $j \in \tilde{B}$ has energy E_j in kJ, a cost C_j in financial units, a weight w_j in kg, and a decision variable b_{ji} that is 1 if battery type j is in the UAV at location i with $z_i \geq 0$, and 0 otherwise. In eq(70), the continuous battery weight z_i/ϵ at location i can be replaced with the weight of the chosen batteries $\sum_{j \in \tilde{B}} w_j b_{ji}$. In eq(77), the continuous total cost $\epsilon \sum_{i \in N_0} z_i$ of batteries can be replaced with the total cost of the chosen batteries $\sum_{i \in N_0} \sum_{j \in \tilde{B}} C_j b_{ji}$. To ensure that the chosen batteries' energy is adequate, constraint $\sum_{j \in \tilde{B}} E_j B_{ji} \geq z_i \quad \forall i \in N_0$ can be added.

Problem Formulation

- The problem for minimising the cost of operation can be expressed as

$$\begin{aligned} & min \quad c \\ s.t \quad & eq(57) - eq(78) \end{aligned} \tag{79}$$

3.3.2 Online path planning

Online path planning also known as local path planning is a scheme where the path is generated by taking data from the sensors/cooperative agents during the movement of the UAV. Therefore, an UAV can generate a new path in response to a new environment/objective. This method is more complicated in design but more applicable in practice. While the UAV is in flight the following scenerios may arrise which then need an online path planning

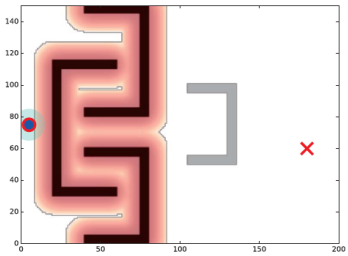

(a) A mission with deterministic (black) and non-deterministic(grey) obstacles

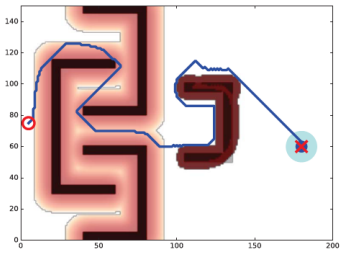

(b) UAV path planning

Figure 16: An online path planning scenerio

- The UAV comes in proximity of an unforseen object/topography
- The UAV gets dissuaded from its path due to unknown environmental factors
- In a cooperative operation, the objective of an UAV changes
- There is an updation of global information map

Online path planning scenerio The following offline path planning scenerio is based on [21]

Problem Statement Given a low altitude dynamic urban environment with a static safety index map, an UAV needs to make its way through the terrain from an origin to a destination autonomously with certain objectives

Objectives

- There is no collision with an unforseen obstacle/terrain
- The travel time is minimised

Solution To this end we need to solve the static preplannig problem offline (from the static safety index map) and a dynamic replanning problem to attend to the unforseen obstacles. The online path planner takes into account the sensing mechanism of the UAV and reroutes the trajectories considering a planning horizon whenever an unknown environment triggers the sensors. The solution is in the form of a pareto optimal path that takes care of the objectives as mentioned above.
For this scenerio, few notions are discussed below

- **Position Uncertainity Model**
  It is assumed that there is uncertainity in the position and navigation system of the UAV, so a position uncertainity model is described to avoid any discrepency in obstacle detection. A bivariate Gaussian model is utilized to simulate the uncertainity in 2-D space. The UAV position density function p can be expressed as

$$p(x_c, y_c, \sigma_x, \sigma_y) = \frac{1}{2\pi\sigma_x\sigma_y} e^{-\left(\frac{(x-x_c)^2}{2(\sigma_x)^2} + \frac{(y-y_c)^2}{2(\sigma_y)^2}\right)} \tag{80}$$

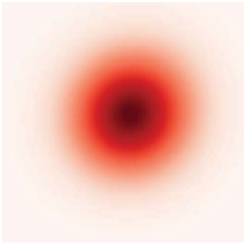

Figure 17: Position uncertainity model

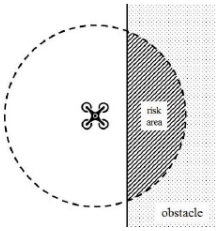

Figure 18: UAV risk area

where σ_x and σ_y are standard deviatins, $s_c = (x_c, y_c)$ is the coordinate of the center point of the position uncertainity model depicted in figure17. Given a normal distribution, $P(\mu - 3\sigma < X \leq \mu + 3\sigma) = 99.7\%$. Similarly this 3σ principle is used to bind the above mentioned probability circle.

- **Risk probability**
  The UAV risk probability refers to the probability that the UAV will hit obstacles due to the position error, which can be denoted by

$$Pr(x_c, y_c) = \int_{\phi \in \Phi} p(x_c, y_c, \sigma_x, \sigma_y) d\phi \tag{81}$$

  where Φ represents the risk area as shown in figure18.
  Alternatively, the safety probability of the UAV located at the center point is calculated using the form

$$\tilde{Pr}(x_c, y_c) = 1 - Pr(x_c, y_c) \tag{82}$$

- **Static Safety Index Map**
  Given a space graph $G = (N, A, c)$, the static SIM describes the UAV flight safety index at an arbitrary point s_c in the space graph, which can be denoted by

$$I(s_c) = -10 \log_{10}(\tilde{Pr}(x_c, y_c)) \tag{83}$$

  It is worth to note that the safety index of a path is the sum of the safety indices of all points on the path, and a greater path safety index indicates a more dangerous path. In realization, the safety indices of the points far away from an obstacle are small, e.g., close to zero in general. Only those of the points near an obstacle contribute to the safety index of a path. Hence, in order to reduce the computational complexity, one may only calculate the probability that a UAV collides with each obstacle on the path instead and obtain the corresponding safety index, which is in fact the summation of the safety indices of all the points near the obstacle.

- **Dynamic Safety Index Map**
  Here a dynamic SIM is constructed to depict the safe and hazardous regions of unexpected obstacles.

  – Perception Range: UAVs need to detect surroundings in performing missions to perceive the surrounding information. Denote R by the sensing distance of onboard sensing sensors; thus, one can define the perceptual range of a UAV

as a circle centered at the UAV, and R is the radius in 2-D space. In other words, the perceptual range of a UAV can take the form

$$(x_c - x)^2 + (y_c - y)^2 = R \tag{84}$$

where, (x, y) is an arbitrary point within the perceptual range. If a UAV detects that obstacles appearing in its perception range are unknown, it will mark these obstacles as unexpected and call the following mechanism to construct a dynamic SIM for them.

– Safety Margin: When a UAV finds an unexpected obstacle appearing in its perception range, one of the obstacle avoidance measures that the UAV can take is emergency braking, which is associated with the speed of the UAV. The braking distance is called the "safety margin" (denoted by d_{sm}) in this paper. Next, the following formation can be utilized to construct the dynamic SIM of unanticipated obstacles:

$$I(s_c) = \begin{cases} +\inf & d_c \leq d_{sm} \\ 0 & \text{else} \end{cases} \tag{85}$$

where, d_c represents the vertical distance between the UAV and the unexpected obstacle.

Path Planning Formulation Here, a multiobjective optimization problem is formulated with two objectives: 1) travel time and 2) safety. The solution of this problem is to find an optimal path p between the source point and target point in a graph $G(N, A, c)$. Each arc i in A has two non-negtive costs denoted by $c_{i,1}$ and $c_{i,2}$ representing the travel time and safety, respectively. Let $g_j(p)$ be the total cost of the whole arcs in a path p for the jth objective. Let $g(p) = (g_1(p), g_2(p))$ be the cost vector for a path p. Therefore, when compared with any other path q the "optimal" path p should meet with the following conditions:

$$g_j(p) \leq g_j(q) \qquad \forall j \in \{1,2\} \quad \text{and} \quad \exists i \in \{1,2\}, g_i(p) < g_i(q) \tag{86}$$

Solutions that are nondominated by any other solutions are the Pareto optimal solutions (denoted by a Pareto set P in this paper). Path p is a Pareto optimal path of the Pareto optimal set, which has the minimal total cost W

$$W = \min_{p \in P} \alpha g_1(p) + (1 - \alpha) g_2(p) \tag{87}$$

3.4 Research Gap

- On a multi-objective path planning scheme, the objective of minimizing energy consumption is avoided in most cases. The cases that consider energy consumption as an objective are grid-based path planning, where the path is assumed as a straight line from one point to the other[26]. The energy consumption modeling can be tested against various types of trajectories and accordingly an optimal/quasi-optimal trajectory can be calculated that would result in the least energy consumption.

- To the best of our knowledge, online path planning is not formulated in the literature when an UAV gets dissuaded from its path due to environmental factors like wind. Consider a case where a UAV is dissuaded from its preplanned path due to external stimuli. The path planning algorithm should be able to replan a trajectory from that instant such that energy is minimized for the rest of the journey.

- To the best of our knowledge, weather data is not taken into consideration during the path planning of an UAV. In civil aviation, a flight plan is designed based on the current weather which may include waypoints that are placed according to the wind directions of the region[27]. Such flight plans aid the flight with minimum fuel burnt against the flow of wind. Similarly in UAV path planning, wind data can be considered for an efficient flight.

4 Conclusion

In this research work, we have addressed two aspects of an Unmanned Aerial Vehicle (UAV), one being the power consumption model that calculates the energy consumed in a trip and other being path planning which results in efficient trips. We have surveyed the literature for both these aspects. Then we have made an attempt to derive a dynamic power consumption model using the angular speeds of rotors. The model however needs to be defined with proper units. The model also needs to be tested against practical power consumption using voltage and current measurements on a real UAV setup. The future prospects of the work is to derive a path planning algorithm which will be applied using our power consumption model. We aim to address the research gaps as mentioned above. Finally we wish to apply path planning with minimal energy consumption in a multi-agent setup.

References

[1] India Brand Equity Foundation(IBEF), "Indian drone industry reaching the skies." [Online]. Available: https://www.ibef.org/blogs/indian-drone-industry-reaching-the-skies

[2] Federation of Indian Chambers of Commerce and Industry (FICCI), "Smart border management-contributing to a 5 trillion dollar economy," 2019.

[3] The Hindu Business Line, "Precision farming and drones can help india make the big leap," May 2021. [Online]. Available: https://www.thehindubusinessline.com/opinion/farming-the-potential-of-drones/article34573234.ece

[4] Ministry of Civil Aviation, Govt. of India, "Drone rules 2021," *The Gazette Of India, Extraordinary, Part II, Section 3, Sub Section(i)*, 2021.

[5] M. A. Uddin, M. Ayaz, E.-H. M. Aggoune, A. Mansour, and D. Le Jeune, "Affordable broad agile farming system for rural and remote area," *IEEE Access*, vol. 7, pp. 127 098–127 116, 2019.

[6] J. Zhang, J. F. Campbell, D. C. Sweeney II, and A. C. Hupman, "Energy consumption models for delivery drones: A comparison and assessment," *Transportation Research Part D: Transport and Environment*, vol. 90, p. 102668, 2021.

[7] Z. Liu, R. Sengupta, and A. Kurzhanskiy, "A power consumption model for multi-rotor small unmanned aircraft systems," in *2017 International Conference on Unmanned Aircraft Systems (ICUAS)*. IEEE, 2017, pp. 310–315.

[8] K. Dorling, J. Heinrichs, G. G. Messier, and S. Magierowski, "Vehicle routing problems for drone delivery," *IEEE Transactions on Systems, Man, and Cybernetics: Systems*, vol. 47, no. 1, pp. 70–85, 2016.

[9] R. D'Andrea, "Guest editorial can drones deliver?" *IEEE Transactions on Automation Science and Engineering*, vol. 11, no. 3, pp. 647–648, 2014.

[10] T. Kirschstein, "Comparison of energy demands of drone-based and ground-based parcel delivery services," *Transportation Research Part D: Transport and Environment*, vol. 78, p. 102209, 2020.

[11] H. Y. Jeong, B. D. Song, and S. Lee, "Truck-drone hybrid delivery routing: Payload-energy dependency and no-fly zones," *International Journal of Production Economics*, vol. 214, pp. 220–233, 2019.

[12] C.-M. Tseng, C.-K. Chau, K. M. Elbassioni, and M. Khonji, "Flight tour planning with recharging optimization for battery-operated autonomous drones," *CoRR, abs/1703.10049*, 2017.

[13] J. K. Stolaroff, C. Samaras, E. R. O'Neill, A. Lubers, A. S. Mitchell, and D. Ceperley, "Energy use and life cycle greenhouse gas emissions of drones for commercial package delivery," *Nature communications*, vol. 9, no. 1, pp. 1–13, 2018.

[14] W. Johnson, *Helicopter Theory*. Dover Publications, 1980.

[15] S. Gudmundsson, *General Aviation Aircraft Designs - Applied Methods and Procedures*. Butterworth-Heinemann, 2013.

[16] P. Corke, *Robotics, Vision and Control: Fundamental Algorithms in MATLAB*. Springer, 2011.

[17] J. Leishman, *Principles of Helicopter Aerodynamics: 12 (Cambridge Aerospace Series, Series Number 12)*. Cambridge, UK: Cambridge University Press, 2002.

[18] U. S. Department Of The Army, *Fundamentals of Flight (FM 3-04.203)*. Washington D.C, US: Army Knowledge Online, 2007.

[19] W. T. Hoffmann, Huang, "Quadrotor helicopter flight dynamics and control: Theory and experiment," *AIAA Guidance, Navigation and Control Conference and Exhibit*, 2007.

[20] C. Zheng, L. Li, F. Xu, F. Sun, and M. Ding, "Evolutionary route planner for unmanned air vehicles," *IEEE Transactions on robotics*, vol. 21, no. 4, pp. 609–620, 2005.

[21] C. Yin, Z. Xiao, X. Cao, X. Xi, P. Yang, and D. Wu, "Offline and online search: UAV multiobjective path planning under dynamic urban environment," *IEEE Internet of Things Journal*, vol. 5, no. 2, pp. 546–558, 2017.

[22] P. P.-Y. Wu, D. Campbell, and T. Merz, "Multi-objective four-dimensional vehicle motion planning in large dynamic environments," *IEEE Transactions on Systems, Man, and Cybernetics, Part B (Cybernetics)*, vol. 41, no. 3, pp. 621–634, 2010.

[23] V. Roberge, M. Tarbouchi, and G. Labonté, "Comparison of parallel genetic algorithm and particle swarm optimization for real-time UAV path planning," *IEEE Transactions on industrial informatics*, vol. 9, no. 1, pp. 132–141, 2012.

[24] K. Sundar and S. Rathinam, "Algorithms for routing an unmanned aerial vehicle in the presence of refueling depots," *IEEE Transactions on Automation Science and Engineering*, vol. 11, no. 1, pp. 287–294, 2013.

[25] A. Koubaa, *Unmanned Aerial Systems - Theoritical Foundations and Applications*. Elsevier, 2021.

[26] R.-J. Wai and A. S. Prasetia, "Adaptive neural network control and optimal path planning of UAV surveillance system with energy consumption prediction," *IEEE Access*, vol. 7, pp. 126 137–126 153, 2019.

[27] W.-X. Lim and Z.-W. Zhong, "Re-planning of flight routes avoiding convective weather and the "three areas"," *IEEE Transactions on Intelligent Transportation Systems*, vol. 19, no. 3, pp. 868–877, 2017.